Chinese Journal of Polymer Science Vol. 33, No. 3, (2015), 444–455

Chinese Journal of Polymer Science

Thermal, Mechanical and Rheological Properties of Biodegradable Poly(propylene carbonate) and Poly(butylene carbonate) Blends*

Dan-dan Wu[a, b], Wu Li[a, b], Yan Zhao[a, b], Yun-jiao Deng[a], Hui-liang Zhang[b**], Hui-xuan Zhang[a] and Li-song Dong[b]

[a] *Changchun University of Technology, Changchun 130012, China*

[b] *Laboratory of Polymer Ecomaterials, Chinese Academy of Sciences, Changchun Institute of Applied Chemistry, Changchun 130022, China*

Abstract Poly(propylene carbonate) (PPC) was melt blended in a batch mixer with poly(butylene carbonate) (PBC) in an effort to improve the toughness of the PPC without compromising its biodegradability and biocompatibility. DMA results showed that the PPC/PBC blends were an immiscible two-phase system. With the increase in PBC content, the PPC/PBC blends showed decreased tensile strength, however, the elongation at break was increased to 230% for the 50/50 PPC/PBC blend. From the tensile strength experiments, the Pukanszky model gave credit to the modest interfacial adhesion between PPC and PBC, although PPC/PBC was immscible. The impact strength increased significantly which indicated the toughening effects of the PBC on PPC. SEM examination showed that cavitation and shear yielding were the major toughening mechanisms in the blends subjected the impact tests. TGA measurements showed that the thermal stability of PPC decreased with the incorporation of PBC. Rheological investigation demonstrated that the addition of PBC reduced the value of storage modulus, loss modulus and complex viscosity of the PPC/PBC blends to some extent. Moreover, the addition of PBC was found to increase the processability of PPC in extrusion. The introduction of PBC provided an efficient and novel toughened method to extend the application area of PPC.

Keywords: Biodegradable; Poly(propylene carbonate); Poly(butylene carbonate); Blends.

INTRODUCTION

Recently, much effort has been devoted to developing biodegradable and renewable resource-derived polymers because of the worldwide environment concerns and sustainability issues resulted from petroleum-based polymers. Biodegradable polymers offer a promising alternative to petroleum-based polymers that are renewable, environmental friendly and can be readily degraded in a natural environment. Carbon dioxide copolymers, the copolymers of carbon dioxide and epoxides, are materials with great industrial interests because of the fixation of carbon dioxide and the biodegradability[1]. In 1969, Inoue *et al.* first observed that the copolymerization of CO_2 with epoxides could from aliphatic polycarbonates using organometallic compounds as catalysts under relatively mild conditions[2]. Since then, much work has been done to make carbon dioxide copolymers with other monomers[3, 4]. Poly(propylene carbonate) is a kind of linear aliphatic polyester *via* the copolymerization of carbon dioxide and propylene oxide[5, 6]. PPC is a biodegradable aliphatic polycarbonate that can be degraded to H_2O and CO_2. The utilization of CO_2 as one of the synthetic monomers can largely reduce the

* This work was financially supported by the fund of Science & Technology Bureau of Jilin Province of China (No. 20126023), the National High Technology Research and Development Program of China (863 Program) (No. 2012AA062904) and the National Natural Science Foundation of China (No. 51021003).

** Corresponding author: Hui-liang Zhang (张会良), E-mail: hlzhang@ciac.jl.cn

Received June 4, 2014; Revised June 27, 2014; Accepted July 29, 2014
doi: 10.1007/s10118-015-1597-z

dependence on petroleum resources and the emission of CO_2 contributing to the greenhouse effect. Owing to biodegradability and thermoplasticity, PPC has been processed into biomedical and packing materials. Nevertheless, the flexible carbonate groups in backbone chains have created many blemishes, including lower glass transition temperature, non-crystallizability, weaker processing stability and poor mechanical properties, which are the major drawbacks preventing it from widely practical applications. The blending of different polymers is a simple and economical method to enhance the properties of a polymer matrix[7, 8]. Numerous works has been devoted to improve the thermal and mechanical properties of PPC by blending it with other polymers or inorganic fillers[9–25]. In general, when the softer component forms a second phase within the more brittle continuous phase it may act as a stress concentrator which enables ductile yield and prevents brittle failure.

Poly(butylene carbonate) (PBC)[26–29] is a typical chemosynthetic aliphatic polyester, which is considered the most promising material with high performance and environmentally friendly biodegradable plastics for biomedical and environmental applications, because of its favorable comprehensive properties and low cost. PBC can be synthesized by polycondensation of PBC oligomer or by transesterification between dimethyl carbonate and 1,4-butanediol in the presence of a heterogeneous catalyst. Poly(butylene carbonate) is a semicrystalline polymer with a clear melting point at around 60 °C as well as a glass transition temperature at about −38 °C. PBC is a biodegradable aliphatic polycarbonate and its final degradation products are 1,4-butanediol, carbon dioxide, and di(4-hydroxybutyl) carbonate. The chemical structure of PBC is shown in Fig. 1. PBC possesses excellent impact resistance and satisfactory tensile strength because of the flexibility of its chains with a degradation cycle of half a year. The PBC supplied by our collaborator is a flexible plastic with excellent impact strength and melt processibility. According to literature, PLA was melt blended with PBC which enormously improved the toughness of the PLA[29]. Our overall goal is to produce blends of PPC and PBC with the desired properties and biodegradability. PBC were used to improve the mechanical properties of PPC and the impact strength of PPC could be significantly improved by PBC.

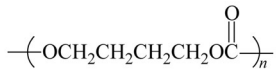

Fig. 1 Chemical structure of PBC

EXPERIMENTAL

Materials

PPC was supplied by Inner Mongolia Mengxi High-tech Materials Co. (China). The number average molecular weight (M_n) and polydispersity index of the purified PPC were determined by GPC as 2.61×10^5 g/mol and 1.36, respectively. PBC used in this study was kindly provided by our collaborator (Institute of Chemistry, Chinese Academy of Science), it had a weight-average molecular weight of 1.23×10^5 g/mol and polydispersity index of 1.81.

Sample Preparation

PPC and PBC were dried at 40 °C for 24 h in a vacuum oven before processing. PPC/PBC blends were prepared by melt mixing with a Haake Rheomix 600 (Karlsruhe, Germany) at a rotating speed 60 r/min at 160 °C for 5 min. The mixing compositions of the PPC/PBC blends were 90/10, 80/20, 70/30, 60/40 and 50/50 *W*/*W*. Also, pure PPC and PBC were subjected to the same mixing treatment so as to obtain reference materials for comparison with the blends. After mixing, all of the compounds were cut into small pieces. Then, all of samples were compression-molded into sheets with thicknesses of 1.0 and 4.0 mm for various tests at 160 °C with a hold pressure of 10 MPa and a hold time of 3 min, followed by quenching to room temperature between two thick-metal blocks kept at room temperature. The specimens were then sealed in plastic bags awaiting the processing and analysis.

Dynamic Mechanical Properties

Dynamic mechanical properties of the blends were studied with a Perkin-Elmer 7 DMA equipment with the aim

to evaluate the possible changes in glass transition temperatures induced by compatibilization. The temperature range studied was from −70 °C to 65 °C at the heating rate of 3 K/min, and the frequency was 1 Hz.

Mechanical Properties Testing

The uniaxial tensile tests were carried out on an Instron 1121 testing machine (Canton MA). Specimens (20 mm × 4 mm × 1 mm) were cut from the previously compression-molded sheets into a dumbbell shape. All tests were conducted at a cross-head speed of 50 mm/min at room temperature according to ASTM D638-2008. At least five specimens for each sample were measured to get an average value.

Notched Izod impact tests were performed at (23 ± 2) °C according to ASTM D256-2010 on an impact testing machine (CEAST, Chengda, China). Specimens (63.2 mm × 12.0 mm × 4.0 mm) were obtained by compression-molding. The notch was milled in having a depth of 2.54 mm, an angle of 45^{o} and a notch radius of 0.25 mm. At least five samples of each type were drawn to fracture.

Morphological Observation

The morphology of the blends was observed by field-emission scanning electron microscopy (SEM) (JSM-5600, JEO LEOL Ltd., Tokyo, Japan) at an accelerating voltage of 15 kV. A layer of gold was sputter-coated uniformly over all of the fractured surfaces before SEM observations.

Thermal Stability

Thermogravimetric analysis (TGA) was performed using a Netzsch STA 409 PC simultaneous thermal analysis instrument. All samples with weight of (10 ± 0.2) mg were heated from room temperature to 800 °C at 10 K/min under nitrogen.

Neat PPC and 70/30 PPC/PBC blend were subjected to TGA in a nitrogen atmosphere. The experiments were conducted at five different heating rates (5, 10, 20, 30 and 40 K/min) from room temperature to 800 °C.

Rheological Properties

Rheological measurements of the samples were carried out on a Physica MCR 2000 rheometer (AR 2000ex USA). Frequency sweep for the all samples was carried out under nitrogen using 25 mm plate-plate geometry. The gap distance between the parallel plates was 0.9 mm for all tests. The sheet samples were about 1.0 mm in thickness. To guarantee that the results of the dynamic rheology tests would lie in the linear visco-elastic zone, the dynamic strain sweep was first conducted to determine a common linear region up to 100% strain at 0.5 rad/s. Based on these experiments, the strain was fixed at 1.25% because this value was located well inside the linear viscoelastic zone. Then the dynamic frequency sweep was carried out over a frequency range of 0.1–100 rad/s. The temperature was set at 160 °C.

RESULTS AND DISCUSSION

Miscibility

The loss tangent tanδ of neat PPC, neat PBC and the PPC/PBC blends were measured by DMA, and the curves are shown in Fig. 2. As for PPC/PBC blends, the DMA curves exhibited two glass transition temperature: the transition temperature at around −23 °C corresponded to the glass transition temperature of PBC, and the glass transition temperature at around 39 °C corresponded to the glass transition temperature of PPC. The T_g of PPC almost did not change with increasing PBC content in the PPC/PBC blends, suggesting that PPC and PBC were immiscible.

Mechanical Properties

Fracture behavior of the specimen in the tensile tests changed from brittle fracture of the neat PPC to ductile fracture of the blends. Figure 3 showed the stress-strain curves of neat PPC and PPC/PBC blends. It can be seen that neat PPC is a brittle polymer. Neat PPC was very rigid and brittle with tensile strength around 37.5 MPa, and the elongation at break only about 3.6%. Neat PPC showed a distinct yield point (maximum load) with subsequent failure by neck instability. On the contrary, all blends showed distinct yielding and stable neck growth through cold drawing. The samples were finally broken at an increased elongation and the elongation

continuously increased with increasing PBC content. In addition, it was interesting to notice that even at 10% of PBC, the elongation of the blend was meaningfully increased, whereas the tensile strength still remained as high as 31.4 MPa.

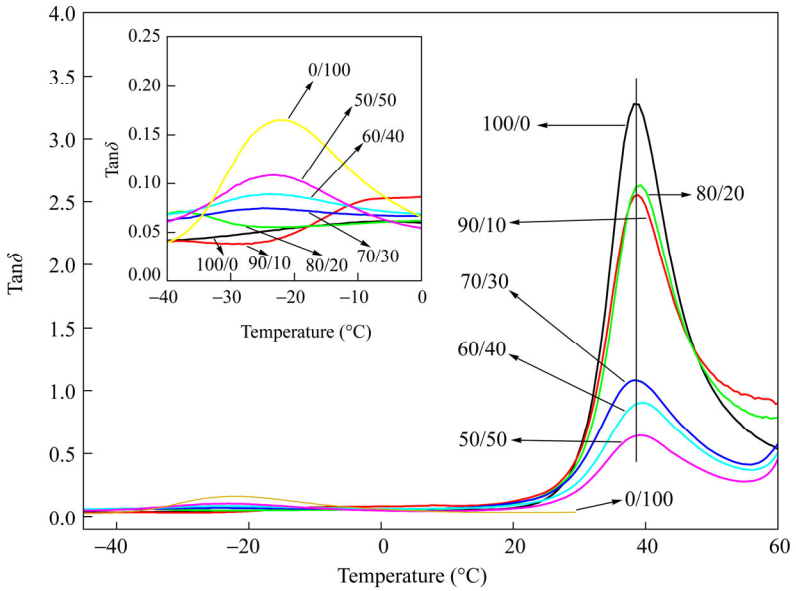

Fig. 2 Tanδ versus temperature traces of neat PPC, neat PBC, and the PPC/PBC blends

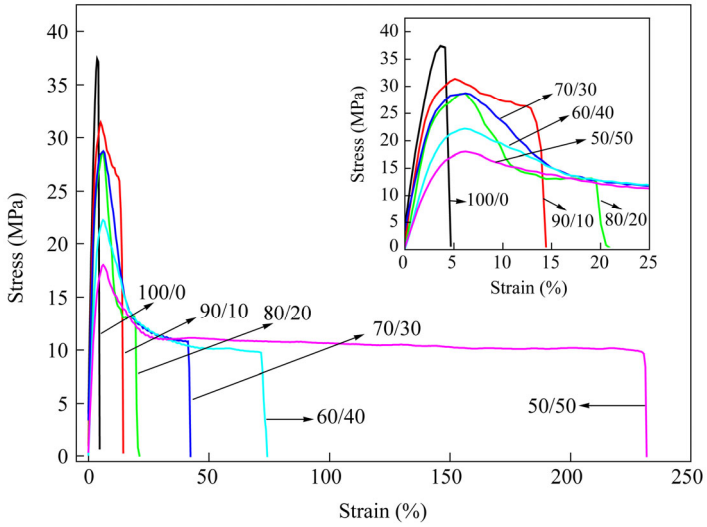

Fig. 3 Tensile stress-strain curves of the PPC/PBC blends

Interfacial interaction between the fillers and matrix is an important factor affecting the mechanical properties of the composites. Thus, theoretical tensile yield strength and ultimate tensile strength of the composites are modelled for the cases of adhesion and no adhesion between the filler particles and matrix. In the case of no adhesion, the interfacial layer cannot transfer stress. The tensile strengths of the composites can be predicted using Pukanszky models[29–31], Eqs. (1) and (2), respectively.

When the interfacial adhesion is strong enough for stress transfer to occur between two phases, the yield stress obeys the law of mixtures:

$$\sigma_b = \sigma_1\phi_1 + \sigma_2\phi_2 \quad (1)$$

where b is the blend, σ is the yield stress and subscripts 1 and 2 refer to component 1 (PPC) and component 2 (PBC), respectively. While in the case of lack of interfacial adhesion, the dispersion of the minor component only results in a reduction of the load-bearing cross section of the matrix. The yield stress is then calculated with Eq. (2):

$$\sigma_b^0 = \sigma_m \frac{1-\phi_d}{1+2.5\phi_d} \quad (2)$$

where superscript 0 denotes zero interfacial adhesion, subscript m is the matrix or continuous phase, and d is the dispersed phase. Figure 4 compares the experimental data with the predictions for extreme interfacial adhesion. The solid line was plotted with Eq. (1) (strong interfacial adhesion), whereas the dotted line was plotted with Eq. (2) (no interfacial adhesion). The PPC/PBC blends had a significant postitve deviation with respect to the predications by Eq. (2). The Pukanszky model gave credit to modest interfacial adhesion between PPC and PBC, although PPC/PBC was an immscible blend. The interfacial adhesion has a great influence in the micromechanical deformation process. When there is not adequate inferfacial adhesion, the micromechanical deformation process is initiated with debonding[32, 33].

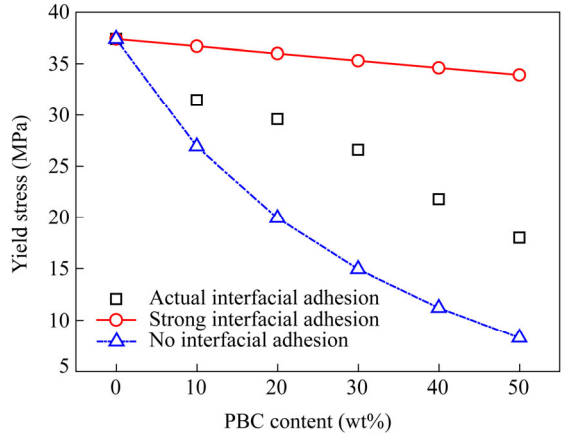

Fig. 4 Yield stress versus the composition for PPC/PBC blends

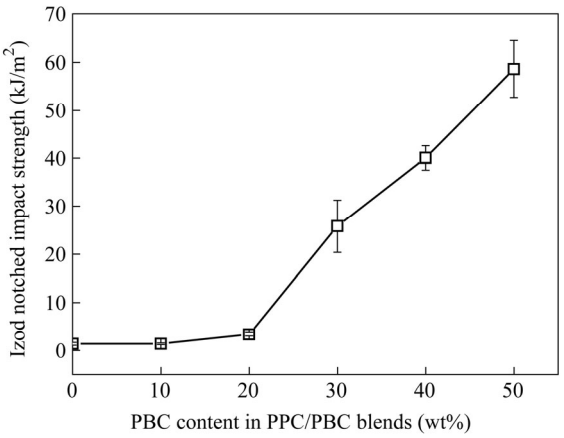

Fig. 5 Notched impact strength of PPC/PBC blends

Figure 5 illustrates the notched Izod impact strengths of PPC/PBC, which indicated that the PBC generated a significant improvement on the impact strength of the blends compared with PPC. The impact strength of pure PPC was 1.4 kJ/m^2, whereas the impact strength of the 50/50 PPC/PBC blend was 58.6 kJ/m^2. The brittle-ductile transition of the blends was obtained when the PBC contents varied from 20 wt% to 30 wt%.

Morphology Observation

In impact tests, the difference between brittle and ductile fracture can be distinguished from the fracture surface of the samples. On a brittle fracture surface stress whitening can only be observed at the origin of the notch tip, but for a tough fracture, all the materials around the fracture surface is involved in stress whitening and a yielded zone is formed. SEM micrographs of impact-fractured surface of PPC/PBC blends are shown in Fig. 6. From them the clear differences of deformation was observed. Figures 6(b) and 6(c) show a flat area close to the blunt notch, which revealed that the fracture was brittle. For those blends, the stress whitening could only be seen from the notch tip, and there was no yielded zone on its fracture surface. Because of the lack of phase adhesion, debonding can easily take place at the particle matrix interface. During the fracture process many domains of the minor phase of PBC were pulled away from the matrix phase of PPC, which remained as empty holes. The

micrographs taken in the impact-fractured surfaces revealed that the stress whitening was a result of the rubber particles debonded at the matrix/particle interface. Voiding, indicative of ductile tearing, was easily observed on the fractured surface (as Fig. 6d). When the content of PBC reached above 40 wt% in the blends, large numbers of voids with shear flow were observed on the fractured surface (as Figs. 6e and 6f), which was the important energy-dissipation process leading to a toughened, biodegradable polymer blend.

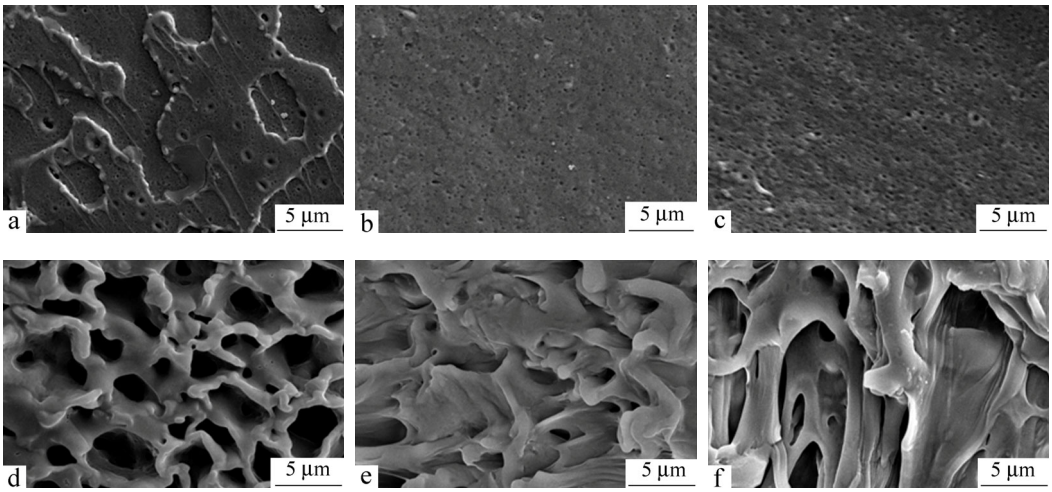

Fig. 6 Micrographs of impact-fractured surfaces of the PPC/PBC blends: (a) neat PPC, (b) 90/10, (c) 80/20, (d) 70/30, (e) 60/40 and (f) 50/50

In order to correlate the external morphology of the ductile fracture surface to the internal deformation mechanisms of the yielded zone, the 50/50 PPC/PBC blend was chosen for SEM analysis. Figure 7 provides schematic preparation of samples used for examination of deformation mechanisms in PPC blends by using SEM. The gray areas represent the deformation region[34].

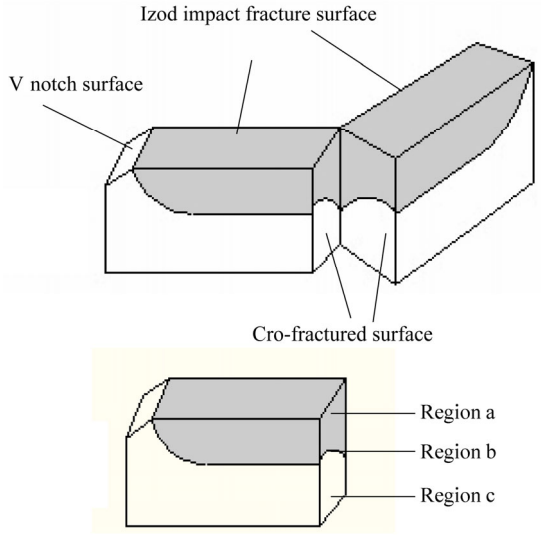

Fig. 7 Schematic presentation of the preparation of samples used for examination of deformation mechanisms in PPC/PBC blends by using SEM (The gray areas represent the deformation region.)

A number of scanning election micrographs were obtained through the sample as defined in Fig. 7, and the sections were taken at different distances from the fracture surface. The sample for SEM observation was

prepared by cryogenically splitting the stress-whitening zone of the blend, after immersion in liquid nitrogen for 20 min[35].

It can be seen that the stress-whitening zone is cavitated (as Fig. 8a), while outside the stress-whitening zone it does not happen at all (as Fig. 8c). Cavitation could occur inside the rubber particles or at the interface between the rubber particles and the polymer matrix. As it has been discussed above, because there was no sufficient interfacial adhesion between PBC and PPC, instead of cavitation within the PBC core under the stress, interfacial debonding took place. Furthermore, cavitation should occur accompanied by other processes. With the debonding progress, the PPC matrix stranded between PBC particles deformed more easily to achieve the shear yielding. These cavities were deformed and the matrix around the sheared rubber particles had plastically deformed to a similar degree (as Fig. 8b)[36], thus the morphology further proved the occurrence of shearing yielding of the PPC matrix. For the blend, the cavitation prevents hydrostatic tension, encourages shear deformation in the surrounding matrix, and thus produces extensive local ductility. This toughening mechanism was in agreement with the findings in other systems[32, 33, 37]. Fracture morphology showed cavitation and shear yielding of the PPC matrix which were the major toughening mechanisms.

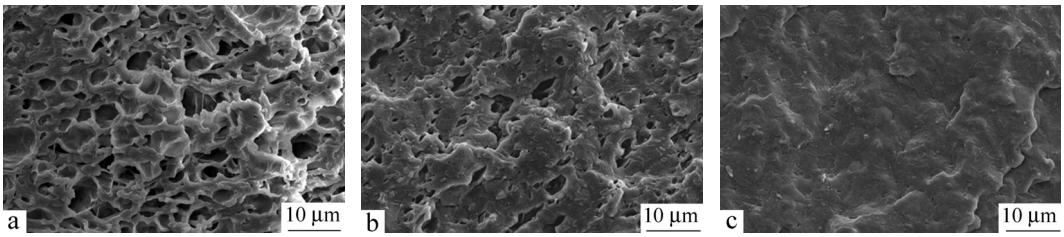

Fig. 8 SEM micrographs in the deformation zone of PPC/PBC 50/50 blend (The location of the observed surfaces is illustrated in Fig. 7.)

Thermal Stability

Thermal stability is of particular importance for any materials in the melting-process. The TGA trace for PPC, neat PBC and PPC/PBC blends under nitrogen flow is shown in Fig. 9. The corresponding characteristic temperatures are given in Table 1. The thermal degradation behavior of PPC, neat PBC and the blends with changing composition were compared using the 5% weight loss temperature ($T_{5\%}$) and the temperature corresponding to the maximum rate of mass loss (T_{max}) in order to explain the effects of PBC on the thermal degradation process of PPC. The $T_{5\%}$ of PPC started at 258 °C. After that, there was a quick weight loss, and the T_{max} occured at 277 °C. The $T_{5\%}$ of PPC/PBC blends tended to decrease with increasing PBC content. The thermal degradation process of all blends had two stages in the temperature range of 230–270 °C and 270–370 °C. The first stage might belonged to the degradation of PPC and the second stage was the degradation of PBC. At the temperatures higher than 370 °C, PPC decomposed completely. The $T_{5\%}$ and T_{max} of the PPC/PBC blends decreased slightly compared with those of the PPC matrix. Both $T_{5\%}$ and T_{max} showed that the thermal stability of PPC decreased with the incorporation of PBC.

The activation energy of decomposition, E_t, of the polymer can be calculated from the TGA curves by Flynn-Wall-Ozama method[38]:

$$\lg \beta = \lg \frac{AE}{RF(\partial)} - 2.315 - 0.457 \frac{E}{RT} \tag{3}$$

where β is the heating rates, ∂ is the fractional conversion, $F(\partial)$ is the reaction mechanism function and has nothing to do with the temperature, E is the activation energy of decomposition, A is the pre-exponential factor, T is the absolute temperature and R is the gas constant. From the plots of $\lg\beta$ versus T^{-1}, which are shown in Fig. 10. E can be determined from the slope of the straight line of the plots.

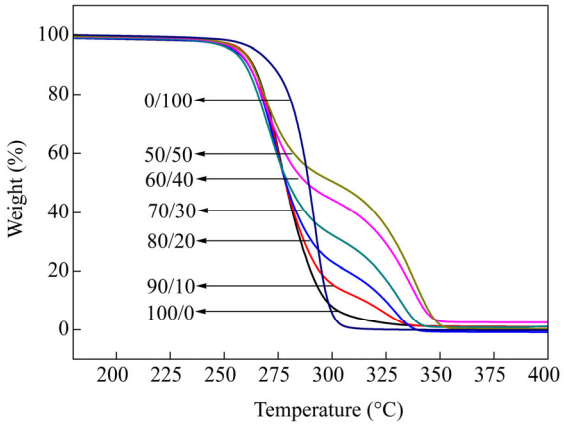

Fig. 9 The TGA curves of PPC and PPC/PBC blends

Table 1. Character temperatures of TGA curves

PPC/PBC (*W*/*W*)	$T^1_{5\%}$ (°C)	T^1_{max} (°C)	T^2_{max} (°C)
100/0	257.9	276.8	–
90/10	257.9	275.3	324.8
80/20	254.5	273.6	328.3
70/30	253.3	270.5	331.8
60/40	255.5	269.5	337.6
50/50	257.3	269.1	338.7
0/100	264.6	–	292.1

T^1_{max} and T^2_{max} were denoted as the thermal decomposition temperature with the max rate of the PPC-rich phase and PBC-rich phase, respectively.

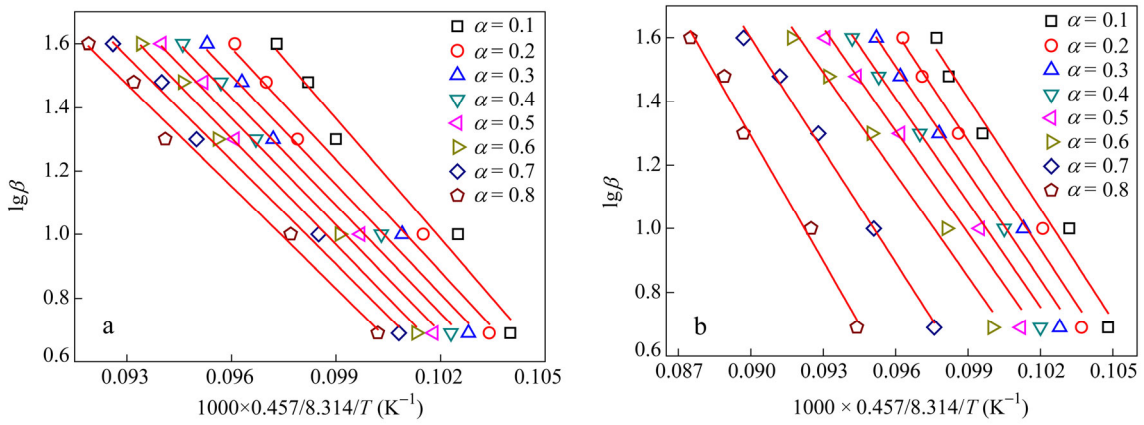

Fig. 10 Flynn-Wall-Ozama plots at the following different weight loss of (a) neat PPC and (b) 70/30 PPC/PBC

The thermal degradation kinetic analysis of PPC and 70/30 PPC/PBC blend were determined with Flynn-Wall-Ozama method. The Flynn-Wall-Ozama plots are shown in Fig. 10. Figure 10 shows that the fitting lines are straight lines with a relatively good correlation coefficient *r*, which indicates the applicability of Flynn-Wall-Ozama to the systems in the conversion range investigated. The *E* values of samples are shown in Table 2. The thermal degradation process of the blend had two stages, the *E* at the initial stage of the degradation (before 70% conversion) decreased just as the degradation trend of neat PPC. After that, the *E* of the blend was higher than that of pure PPC at the same weight loss. It could be inferred that the addition of PBC caused the early degradation due to the decreased *E*.

Table 2. Activation energies of neat PPC and 70/30 PPC/PBC blend determined by Flynn-Wall-Ozawa method method

Conversion ∂	PPC E (kJ/mol)	PPC/30%PBC E (kJ/mol)
0.1	126.2	116.4
0.2	117.4	114.2
0.3	114.5	111.9
0.4	113.0	109.4
0.5	112.5	107.7
0.6	111.8	107.2
0.7	109.0	117.6
0.8	107.3	131.5

Rheology

The rheological behavior of molten polymers is of great importance because it is related to their microstructure and governs their processing characteristics. Small-amplitude oscillatory shear experiments were performed to measure the storage modulus (G'), loss modulus (G'') and the complex viscosity (η^*) of the polymer samples as a function of angular frequency (ω), which is related to the elastic and viscous characteristics of materials.

Figure 11 describes the relationship between the G', G'' and η^* versus ω for the PPC/PBC blends. It showed viscoelastic behaviors for neat PPC and the PPC/PBC melts, which are combination of irreversible viscous flow due to the polymer chain slippage and reversible elastic deformation due to molecular entanglement.

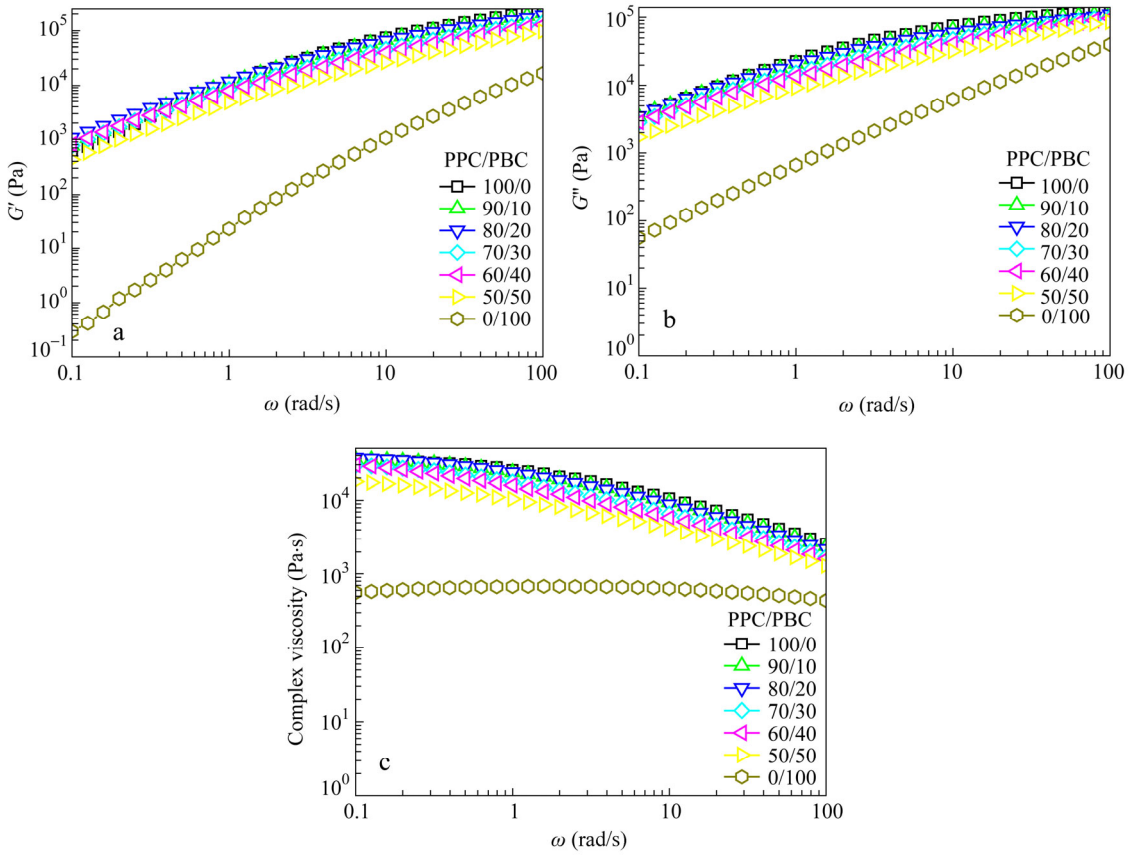

Fig. 11 Deduced frequency dependence of (a) storage modulus G' (ω) (b) loss modulus G'' (ω) and (c) complex viscosity η^* (ω) of PPC matrix and PPC/PBC melts (T = 160 °C.)

As we all know, the G' is related to the elastic behavior of the material and may be considered as the storage energy. The G'' represents the dissipated energy. As shown in Figs. 11(a) and 11(b), although compared with that of the PPC matrix, the G' of the pure PBC was smaller by three orders, the incorporation of PBC had less effect on the G' of melts at the whole frequencies. The G'' of the blends remained largely unaffected with the variation of PBC content. These results were important because they indicated the optimal processing conditions for the blends without sacrificing the melt strength.

The η^* of the samples as a function of frequency is shown in Fig. 11(c). The η^* of neat PPC followed the general behavior of typical thermoplastic polymers, that is, nearly Newtonian behavior at low frequencies and shear-thinning behavior at high frequencies. The zero-shear viscosity was determined to be 34350 Pa·s for PPC. The viscosity of PPC was more than eight times higher than that of PBC at 50 rad/s. It appeared that PBC had a longer Newtonian region than PPC, and the addition of PBC reduced the value of η^* of the blends to some extent. Rheology data indicated a lower viscosity of PBC than that of PPC at 160 °C, the addition of PBC was found to increase the processability of PPC in extrusion. Barrel temperatures were set to a profile during extrusion to reduce thermal impact and minimize polymer degradation. PPC pellets were rigid and very difficult to compress in a screw flute. During extrusion PPC pellets existed in the first few sections of the barrel due to the low-temperature profile. This led to large resistance to melt flow and thus caused high screw torque and extrusion pressure in the pure PPC extrusion. The melting point of PBC was much lower than that of PPC. It melted from the first section of the barrel and then acted as lubricant to help transfer PPC pellets. As such, the screw torque and extrusion pressure were reduced.

The temperature dependence of the viscosity of polymer melts is one of the most important parameters in polymer flow. To express the viscosity-temperature behavior, an Arrhenius-type equation derived by Eyring[39] was used:

$$\eta_0 = Ae^{E_a/RT} \tag{4}$$

where η_0 is the absolute or zero-shear viscosity, A is the constant, T is the absolute temperature, R is the gas constant, and E_a is the flow activation energy. The higher the E_a, the more temperature sensitive is the melt.

The activation energy (E_a) of the blends as well as the neat PPC was defined from the slopes of $\ln(\eta_0)$ plotted versus $1/T$. Determining the precise value of E_a for the samples is not the purpose of the study, and complex viscosity data at $\omega = 0.1$ rad/s (measured in the frequency sweep experiments) are used instead of zero-shear viscosity data and fitted into the equation[40].

$$\lg\left(\eta_{\omega=0.1\ \mathrm{rad/s}}\right) = \ln A + \frac{E_a}{RT} \tag{5}$$

Regression analysis showed that the Arrhenius-type equation was applicable for the samples, the regression coefficient was a high value, and the calculated effective activation energy (E_a) values are shown in Table 3. Values of E_a are calculated by using η_0 data at temperatures of 140, 150, and 160 °C. For each calculation, the correlation coefficient (R^2) is better than 0.98. The results obey Arrhenius model. It was clear that E_a tended to decrease with the introduction of PBC. The results indicated that PPC/PBC melts were easier to flow due to the

Table 3. Rheology characteristics of PPC/PBC melts

Samples	Activation energy (kJ/mol)	Regression coefficient (R^2)
100/0	86.3	0.99
90/10	74.8	0.98
80/20	78.5	0.98
70/30	81.2	0.98
60/40	66.3	0.98
50/50	68.1	0.99
0/100	75.5	0.99

addition of the flexible PBC molecular chains. On the other hand, the less temperature dependence of viscosity of PPC/PBC melts made it easier for the choosing of processing temperatures. PPC/PBC blends have a broad processing temperature window due to the less viscosity sensitivity to temperature.

CONCLUSIONS

PPC and PBC were blended by melt mixing to prepare biodegradable polymer blend materials. From the analysis of DMA, PPC was immiscible with PBC. The mechanical properties of PPC could be improved by the addition of PBC. The elongation at break as well as impact strength of PPC/PBC blends was improved significantly compared with those of neat PPC. A PPC-based material with high toughness was achieved by incorporation of PBC. SEM micrographs reveal that cavitation and shear yielding are the major toughening mechanisms. TGA tests showed that the addition of PBC decreased the thermal stability of PPC. Rheological measurements showed that the addition of PBC reduced the value of storage modulus, loss modulus and complex viscosity of the PPC/PBC blends to some extent. Moreover, the addition of PBC was found to increase the processability of PPC in extrusion.

REFERENCES

1 Zhang, Z.H., Zhang, H.L., Zhang, Q.X., Zhou, Q.H., Zhang, H.F. and Mo, Z.S., J. Appl. Polym. Sci., 2006, 100(1): 584
2 Inoue, S, Koinuma, H and Tsuruta, T., J. Polym. Sci., Polym. Lett. Ed., 1969, 7(4PB): 287
3 Beckman, E.J., Science, 1999, 5404(283): 946
4 Michael, S.S. and Beckman, E.J., Trends. Polym. Sci.,1997, 5(7): 236
5 Tao, J., Song, C.J., Cao, M.F., Hu, D., Liu, L. and Liu, N., Polym. Degrad. Stab., 2009, 94(4): 575
6 Li, J., Sun, C.R. and Zhang, X.Q., Polym. Compos., 2012, 33(10): 1737
7 Yao, M.J., Mai, F. and Deng, H., J. Appl. Polym. Sci., 2011, 120(6): 3565
8 Yao, M., Deng, H., Mai, F., Wang, K., Zhang, Q. and Chen, F., Express. Polym. Lett., 2011, 5(11): 937
9 Zhang, Z.H., Shi, Q., Peng, J., Song, J., Song, J.B. and Chen, Q.Y., Polymer, 2006, 47(26): 8548
10 Chen, L.J., Qin, Y.S., Wang, X.H., Zhao, X.J. and Wang, F.S., Polymer, 2011, 52(21): 4873
11 Jiao, J., Wang, S.J., Xiao, M., Xu, Y. and Meng, Y.Z., Polym. Eng. Sci., 2007, 47(2): 174
12 Zeng, S.S., Wang, S.J., Xiao, M., Han, D.M. and Meng, Y. Z., Carbohyd. Polym., 2011, 86(3): 1260
13 Xing, C.Y., Wang, H.T., Hu, Q.Q., Xu, F.F., Cao, X.J. and You, J.C., Carbohyd. Polym., 2013, 92(2): 1921
14 Chen, L.J., Qin, Y.S., Wang, X.H., Li, Y.S., Zhao, X.J. and Wang, F.S., Polym. Int., 2011, 60(12): 1697
15 Yang, D. Z. and Hu, P., J. Appl. Polym. Sci., 2008, 109(3): 1635
16 Peng, S.W., An, Y.X., Cheng, C., Fei, B., Zhuang, Y.G. and Dong, L.S., J. Appl. Polym. Sci., 2003, 90(14): 4054
17 Chen, X., Wang, S.J., Xiao, M., Han, D.M. and Meng, Y.Z., J. Polym. Res., 2011, 18(4); 715
18 Pang, M.Z., Qiao, J.J., Jiao, J., Wang, S.J., Xiao, M. and Meng, Y.Z., J. Appl. Polym. Sci., 2008, 107(5): 2854
19 Wang, X.L., Du, F.G., Jiao, J., Meng, Y.Z. and Li, Y., J. Biomed. Mater. Res. Part B: Appl. Biomater., 2007, 83B(2): 373
20 Gao, J., Bai, H., Zhang, Q., Gao, Y., Chen, L. and Fu, Q., Express. Polym. Lett., 2012, 6(11): 860
21 Wang, X.Y., Peng, S.W. and Dong, L.S., Colloid. Polym. Sci., 2005, 284(2): 167
22 Li, Y.J. and Shimizu, H., Acs. Appl. Mater. Inter., 2009, 1(8): 1650
23 Ma, X.F., Chang, P.R., Yu, J.G. and Wang, N., Carbohyd. Polym., 2008, 71(2): 229
24 Zhang, H.L., Sun, X.H., Chen, Q.Y., Ren, M.Q., Zhang, Z.H., Zhang, H.F. and Mo, Z.S., Chinese J. Polym. Sci., 2007, 25(6): 589
25 Wu, D.D., Li, W, Liang, H.Y., Liu, S.R., Fang, J.Y., Zhang H.L., Zhang, H.X. and Dong, L.S., Chinese J. Polym. Sci. 2014, 32(7): 914
26 Zhu, W.X., Li, C.C., Zhang, D., Guan, G., Xiao, Y.N. and Zheng, L.C., Polym. Degrad. Stab., 2012, 97(9): 1589
27 Shao, M.L., Chen, L. and Yang, Q.J., Appl. Polym. Sci., 2013, 130(1): 411

28 Wang, X.M., Zhuang, Y.G. and Dong, L.S., J. Therm. Anal. Calorim., 2013, 114(1): 77
29 Wang, X.M., Zhuang, Y.G. and Dong, L.S., J. Appl. Polym. Sci., 2013, 127(1): 471
30 Wang, J., Zheng, L., Li, C., Zhu, W., Zhang, D., Xiao, Y. and Guan, G., Polym. Test, 2012, 31(1): 39
31 Ma, X.F., Yu, J.G. and Wang, N., J. Polym. Sci., Part B: Polym. Phys., 2006, 44(1): 94
32 Wu, J.S., Yee, A.F. and Mai, Y.W., J. Mater. Sci., 1994, 29(17): 4510
33 Kim, G.M., Michler, G.H., Gahleitner, M. and Fiebig, J., J. Appl. Polym. Sci., 1996, 60(9): 1391
34 Sun, S.L., Xu, X.Y., Yang, H.D. and Zhang, H.X., Polymer, 2005, 46(18): 7632
35 Gao, G.H., Zhang, J.S., Yang, H.D., Zhou, C. and Zhang, H.X., Polym. Int., 2006, 55(11): 1215
36 Sun, S.L., Tan, Z.Y., Zhang, M.Y., Yang, H.D. and Zhang, H.X., Polym. Int., 2006, 55(8): 834
37 Jiang, L., Wolcott, M.P. and Zhang, J.W., Biomacromolecules, 2006, 7(1): 199
38 Ozawa, T., Bull. Chem. Soc. Jpn., 1965, 38(11): 1881
39 Gu, S.Y., Zhang, K., Ren, J. and Zhan, H., Carbohyd. Polym., 2008, 74(1): 79
40 Joshi, M., Butola, B.S., Simon, G. and Kukaleva, N., Macromolecules, 2006, 39(5): 1839